SAKARYA ÜNİVERSİTESİ
FEN BİLİMLERİ ENSTİTÜSÜ DERGİSİ

Sakarya University Journal of Science
SAUJS

ISSN 1301-4048 e-ISSN 2147-835X Period Bimonthly Founded 1997 Publisher Sakarya University
http://www.saujs.sakarya.edu.tr/

Title: Spectroscopic Characterization and DFT Calculations on 1H-benzimidazole-2-carboxylic acid monohydrate Molecule

Authors: Emine BABUR ŞAŞ, Songül ÇİFÇİ, Mustafa KURT

Recieved: 2022-04-08 00:00:00

Accepted: 2022-08-09 00:00:00

Article Type: Research Article

Volume: 26
Issue: 5
Month: October
Year: 2022
Pages: 1879-1891

How to cite
Emine BABUR ŞAŞ, Songül ÇİFÇİ, Mustafa KURT; (2022), Spectroscopic Characterization and DFT Calculations on 1H-benzimidazole-2-carboxylic acid monohydrate Molecule. Sakarya University Journal of Science, 26(5), 1879-1891, DOI: 10.16984/saufenbilder.1100391
Access link
http://www.saujs.sakarya.edu.tr/en/pub/issue/73051/1100391

New submission to SAUJS
http://dergipark.gov.tr/journal/1115/submission/start

Sakarya University Journal of Science 26(5), 1879-1891, 2022

Spectroscopic Characterization and DFT Calculations on 1H-benzimidazole-2-carboxylic acid monohydrate Molecule

Emine BABUR ŞAŞ*[1], Songül ÇİFÇİ[1], Mustafa KURT[1]

Abstract

After first determining the optimized geometry of the 1H-benzimidazole-2-carboxylic acid monohydrate (1HBCM) molecule using the B3LYP/6-311+ + G (d, p) basis set, we investigated the spectroscopic properties, electronic properties and optical band gap of the molecule. We presented the fitted values of the vibrational frequencies of the molecule both as a table and as a spectrum and compared them with the experimental data. While the band gap energy (ΔE) values of the molecule were calculated using HOMO and LUMO energies, the optical band gap (Eg) values of the molecule were obtained from the Tauc equation. We have given the Eg values of the molecule calculated for direct and indirect transmission by comparing them with the experimental data. In the article, we have also calculated and presented the data of the 1HBCM molecule such as MEP, Mulliken, and DOS.

Keywords: FT-Raman, FT–IR, optical band gap DFT, MEP.

1. INTRODUCTION

The biological activities of benzimidazole and benzimidazole derivatives, such as anticancer, antiviral, anthelmintic, antimalarial, anti-ulcer, antihistaminic, antioxidant, and antifungal, have been widely reported in the literature [1-3]. Benzimidazole derivatives are also widely used in industrial processes as corrosion inhibitors for metal and alloy surfaces. In this molecule, it is difficult to assign the vibrational modes that occur with respect to the different chemical bonds. Despite these problems, there are always attempts to assign vibrational modes of such molecules [4].

The fact that benzimidazole and its derivatives are used in many fields such as medicine, chemistry, and industry has attracted many researchers. In previous studies, benzimidazoles have also been used in organic semiconductor materials [5] and solar cells [6]. When electron acceptor and electron donor molecules come together, charge transfer complexes are formed [7]. The donor-receptor interactions are determined by the HOMO-LUMO energy difference of the

* Corresponding author: ebsas@ahievran.edu.tr
[1] Kırşehir Ahi Evran University
E-mail: sngl_cifci_cfc@hotmail.com, mkurt@ahievran.edu.tr
ORCID: https://orcid.org/0000-0002-9547-5951, https://orcid.org/0000-0003-3009-3490, https://orcid.org/0000-0001-6040-1189

molecules [8]. In this study, we investigated the electronic, spectroscopic, and optical properties of the 1HBCM molecule using the DFT method. In addition to the HOMO-LUMO energy difference, we used DOS spectra for the interactions between neighboring orbitals. Based on the properties of the semiconductor material, we have investigated the optical band gap values experimentally and theoretically using the Tauc equation [9-10].

2. EXPERIMENTAL

The FT-IR and dispersive Raman spectra of the molecule 1H-benzimidazole-2-carboxylic acid monohydrate (1HBCM) were recorded at room temperature using a Bruker IFS 66/S spectrometer in the range 400–4000 cm^{-1} and a 532 nm laser in the range 3200–100 cm^{-1} using Renishaw/Invia. Since the molecule is an organic molecule, the UV spectrum was recorded with Thermoscientific Evulation 60 s in the range of 200–600 nm in ethanol solution.

3. COMPUTATIONAL DETAILS

The molecular structure of 1HBCM was visualized by the DFT /B3LYP/6 311++G(d,p) method, where the optimized parameter values were determined and compared with X-ray data [11]. Vibrational spectra of the molecule were obtained by this method and the spectra were recorded and compared with experimental FT-IR and dispersive Raman spectra. The thermodynamic properties were studied by the same method and correlation plots were obtained. UV-Vis spectra, MEP, frontier molecular orbital energies were calculated in DMSO, ethanol and vacuum. Optical band gap values were determined using the experimental and theoretical UV spectra and presented with figures.

4. RESULT AND DISCUSSIONS

4.1. Molecular Structure

Having found the minimum energy level of the 1HBCM molecule, the shape and geometrical parameters of the molecule in this state are given in Figure 1 and Table 1. As shown in Table 1, these values were compared with X-ray data [11]. According to the X-ray data, the C1-C2 bond length, which was reported to be 1.393, was calculated to be 1.42 in the 1HBCM molecule and was found to be larger than the other C-C bond lengths. This bond length was calculated to be 1.41 in similar molecules [12, 13]. The C4-C5 bond length, calculated as 1.415, is the largest C-C bond length observed in the X-ray data [11].

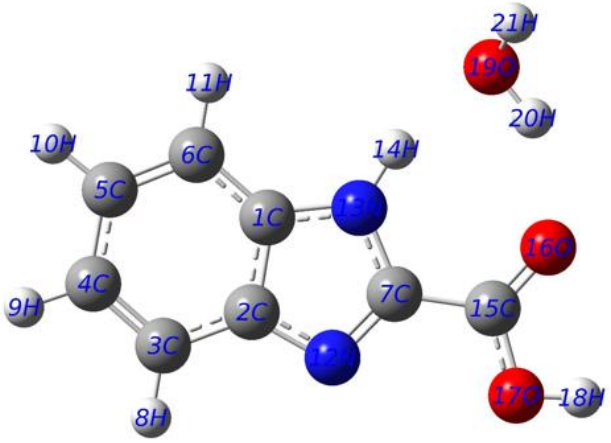

Figure 1 The geometric structure of the 1HBCM

The internal bond angles of the benzene ring in the title molecule are greater or less than the bond angle of a hexagon. For example, the C2-C1-C6 and C1-C6-C5 bond angles were calculated and recorded as 122.2° and 116.3° in 1HBCM and X-ray data, respectively [11]. This difference in bond angles may be due to the imidazole group. This is because the same bond angles are different compared to similar molecules. [12, 13]. The O19-H20 and O19-H21 bond lengths of 1HBCM were calculated to be 0.973 and 0.961 Å, respectively. This bond length was reported to be 0.85 Å in the X-ray data [11].

4.2. Vibrational spectral analysis

The 1HBCM molecule has C1 symmetry and 57 fundamental modes. The fundamental vibration bands of the molecule calculated using the method DFT were fitted with the scaling factors reported in the literature to match the experimental data. A value of 0.958 was used for large frequencies and 0.983 for frequencies below 1700 cm^{-1} [14].

Table 1 Geometrical parameters of 1HBCM and X-Ray data

Bond Lengths (Å)	X-ray	B3LYP/6-311++G(d,p)	Bond angles (°)	X-ray	B3LYP/6-311++G(d,p)
C1-C2	1.393	1.420	C2-C1-C6	122.2	122.2
C1-C6	1.397	1.400	C2-C1-N13	106.9	105.2
C1-N13	1.386	1.371	C6-C1-N13	130.8	132.6
C2-C3	1.393	1.404	C1-C2-C3	121.6	120.1
C2-N12	1.384	1.374	C1-C2-N12	106.0	110.1
C3-C4	1.379	1.383	C3-C2-N12	132.4	129.8
C3-H8	0.936	1.083	C2-C3-C4	116.5	117.8
C4-C5	1.424	1.415	C2-C3-H8	120.0	120.3
C4-H9	1.087	1.084	C4-C3-H8	123.0	121.9
C5-C6	1.367	1.386	C3-C4-C5	121.5	121.5
C5-H10	1.069	1.084	C3-C4-H9	120.0	119.7
C6-H11	0.966	1.083	C5-C4-H9	117.0	118.9
C7-N12	1.335	1.317	C4-C5-C6	121.9	121.9
C7-N13	1.341	1.377	C4-C5-H10	113.0	118.9
C7-C15	1.501	1.472	C6-C5-H10	124.0	119.2
N13-H14	0.900	1.023	C1-C6-C5	116.3	116.6
H14-O19	-	1.873	C1-C6-H11	120.0	121.8
C15-O16	1.254	1.221	C5-C6-H11	124.0	121.5
C15-O17	1.247	1.337	N12-C7-N13	108.9	113.6
O16-H20	-	1.931	N12-C7-C15	125.9	125.9
O17-H18	-	0.969	N13-C7-C15	125.1	120.6
O19-H20	0.850	0.973	C2-N12-C7	109.5	104.7
O19-H21	0.850	0.961	C1-N13-C7	108.6	106.3
			C1-N13-H14	121.0	127.7
			C7-N13-H14	130.0	126.0
			N13-H14-O19	-	162.2
			C7-C15-O16	114.8	124.1
			C7-C15-O17	116.2	113.4
			O16-C15-O17	128.9	122.5
			C15-O16-H20	-	130.7
			C15-O17-H18	-	107.0
			H14-O19-H20	-	88.1
			H14-O19-H21	-	133.2
			H20-O19-H21	107.0	106.9
			O16-H20-O19	-	148.1

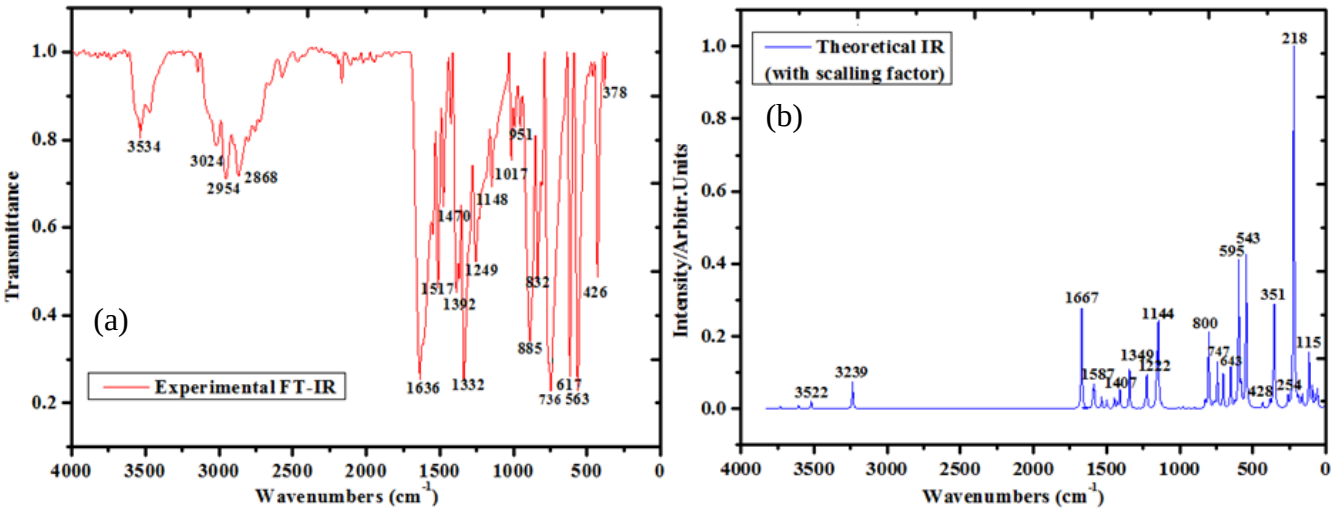

Figure 2 (a) The experimental and (b) the theoretical IR spectra of 1HBCM

The difference between the experimental and theoretical wavenumbers is that the experimental spectra were recorded in the solid phase and the theoretical spectra calculations were performed in the gas phase. The theoretical and experimental spectra are shown in Figure 2 and 3, the values are listed in Table 2.

In molecules an imidazole ring structure, the N-H stretching vibration is generally observed in the range 3500–3000 cm^{-1} [15].

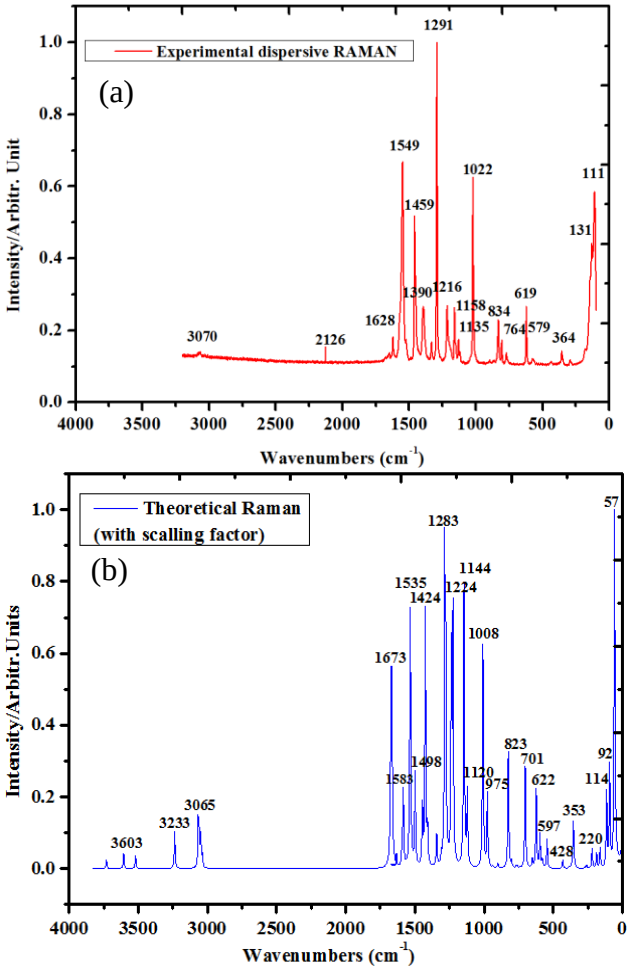

Figure 3 (a) The experimental and (b) the theoretical Raman spectra of 1HBCM

In some similar molecules (2Br1HB, 2-arylaminomethyl-1H-benzimidazole, 2-chloromethyl-1H-benzimidazole hydrochloride, and 2-(4-bromophenyl)-1H-benzimidazole), this vibration is measured above 3500 cm^{-1} at 3546, 3513, 3509, and 3502 cm^{-1}, respectively, and in the 5-benzimidazole carboxylic acid molecule it was measured as 3237 cm^{-1} [12, 16- 19]. This band was calculated as 3236 cm^{-1} in our study and proved to be a pure band according to TED.

In the 1HBCM molecule, C-H vibrations were calculated in the range 3065–3036 cm^{-1} and recorded in the experimental spectrum at the values 3070 cm^{-1} and 3024 cm^{-1}. In aromatic rings, C-H vibrations are observed in the range of 3100–3000 cm^{-1}, in-plane bending vibrations in the range of 1000–1300 cm^{-1} and out-of-plane bending vibrations in the range of 800–950 cm^{-1} [15,20- 22]. These vibrations in the study molecule were calculated in the desired range and presented in detail in Table 2. The correlation graph of the experimental and theoretical wavenumbers given in Table 2 is shown in Figure 4. According to the correlation graph, the R^2 value being 0.99 indicates that the experimental and theoretical data are in agreement.

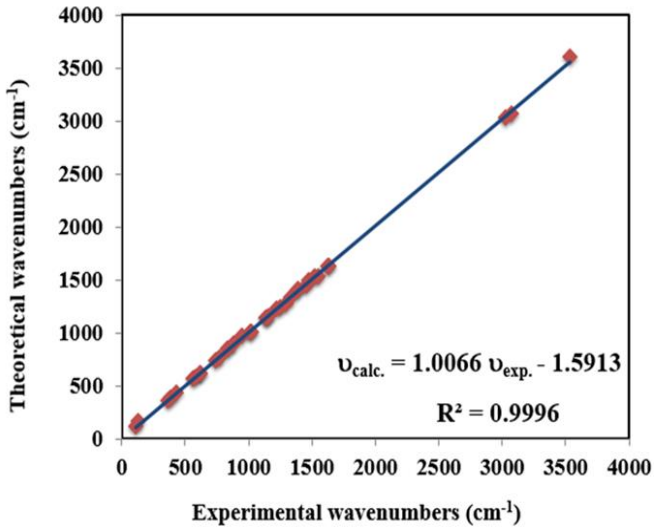

Figure 4 Correlation graphic of calculated and experimental (total) wavenumbers of 1HBCM

C-C, C-N, and C=N vibrations are generally observed to be intermixed. In the literature, these bands are reported to be found in the range of 1480–1650 cm^{-1}, 1338 cm^{-1}, and 1617 cm^{-1}, respectively [23- 25]. For the title molecule, the C-C vibrations were calculated to occur at 1633–1499, 1446–1343, 1281–1224, 1120–975 cm^{-1}, and the C-N and C=N vibrations at 1534–1446, 1408, 1308–1224, 975 cm^{-1}. The highest contribution was calculated as 55% for C-C vibrations at 1633 cm^{-1} and 45% for C-N and C=N vibrations at 1446 cm^{-1}. C-C vibrations were observed experimentally in dis-Raman and FT-IR

in 1628, 1549, 1390, 1291, 1216, 1022 cm^{-1}, and 1636, 1517, 1470, 1392, 1332, 1249 1017 cm^{-1}, respectively. C-N and C=N stretching vibrations were also obtained in 1459, 1390, 1291, 1216 cm^{-1} in dis-Raman and 1517, 1470, 1392, 1249 cm^{-1} in FT-IR.

Table 2 The wavenumbers of 1H-Benzimidazole-2-Carboxylic Acid Monohydrate molecule.

	Theoretical wavenumber				Experimental wavenumber		Assignments TED[a] (≥10%)
No	Scaled	I_{IR}	S_{Ra}	I_{Ra}	IR	Raman	
4	114	10.1	1.4	12.19		111	υOH(13)+δNOH(58)+ δCNH(12)
5	161	3.5	0.5	2.67		131	δOH[δNOH(11)]+ υOH(83)
11	356	34.1	2.6	3.49		364	ɣOH[τCNOH(42)]+ ɣHOH(11)+υCC(13)
16	571	2.0	0.2	0.14	560		τCCCC(40)+τCCCN(16)+τCCCH(15)
17	579	21.8	0.9	0.57		579	δCCC(34)+ δCOO(11)
19	623	6.3	10.9	6.39	616	619	υCC(21)+δCCN(34)+ δCCC(21)
22	741	71.6	0.1	0.03	746		ɣCH[τCCCH(60)+ τCNCH(15)]
24	766	8.6	0.5	0.20		764	τCNCO(39)+τCOOH(19)+τNOHH(15)
26	824	13.9	24.1	9.42	829	834	υCC(55)+ υCN(12)
28	900	2.9	1.3	0.43	889		υCN(14)+δCCC(47)+ δCCH(17)
30	968	0.0	0.2	0.07	956		ɣCH[τCHCH(65)+τCCCH(18)]
32	1008	4.2	64.9	18.79	1011	1022	υCC(54)+δCCH(19)
34	1144	245.4	101.9	24.26	1149	1135	υCO(23)+δCCH(39)+ δCOH(13)
35	1156	145.6	4.3	1.01		1158	υCO(28)+δCCH(22)+ δCOH(15)
36	1224	111.5	102.1	21.84	-	1216	υCN(28)+ υCC(12)+ δCOH(18)
37	1236	20.4	87.0	18.29	1252		υCN(22)+ υCC(14)+ δCCH(29)
38	1281	2.1	246.0	48.87		1291	υCN(42)+ υCC(19)+ δCCH(18)
40	1343	149.9	15.8	2.90	1334		υCC(53)+ δCOH(15)
41	1408	79.2	18.6	3.15	1386	1390	υCO(10)+υCN(17)+ υCC(20)+ δCNH(12)
43	1446	44.9	33.8	5.47	1469	1459	υCN(45)+ δCCH(15)
45	1534	56.5	201.7	29.44	1547	1549	υCC(20)+ υCN(16)+ δCNH(19)
48	1633	1.2	10.0	1.30	1634	1628	υCC(55)
50	3036	1.5	51.8	1.63	3021		υCH(100)
53	3065	10.8	255.1	7.83		3070	υCH(99)
54	3236	726.3	210.5	5.48			υNH(101)
56	3606	139.8	136.3	2.49	3536		υOH(100)

[a]υ: stretching. δ: bending.δ:in plane bending.γ: out of plane bending.Γ: torsion

4.3. UV-Vis Analysis and Optical Band Gap

UV spectrum analysis of the 1HBCM molecule was performed in 2 different solvents (DMSO and ethanol) and in the gas phase. The spectrum obtained experimentally in ethanol is compared theoretically with the spectrum obtained in ethanol and these spectra are shown in Figure 5.

According to Fig. 5, the experimental values were observed at 314, 298, and 291 nm and the theoretical values observed as a shoulder of 1 peak were observed as two peaks at 312 and 293 nm. Although the theoretical absorption peak is calculated at 256 nm in the spectrum, the intensity of this transition is feeble. The theoretical and experimental absorption peak values are very close to each other. The wavelengths of the absorption bands determined experimentally and theoretically are given in Table 3 with the corresponding energies for this transition.

UV spectra are commonly used to investigate a molecule's optical band structure (direct and indirect band gap). Using the Tauc model, we investigated the optical band gap (Eg) of the 1HBCM molecule. Figures 6 show the optical band gaps of the molecule, both theoretically and experimentally. The slope of the graph was used to calculate the Eg values using the Tauc equation. The theoretical and experimental values for the direct optical band gap were 4.12 and 3.68 eV, respectively, as shown in Figure 6, while the indirect band gap was 4.09 and 3.57 eV. The

values obtained experimentally show that the material has semiconductor.

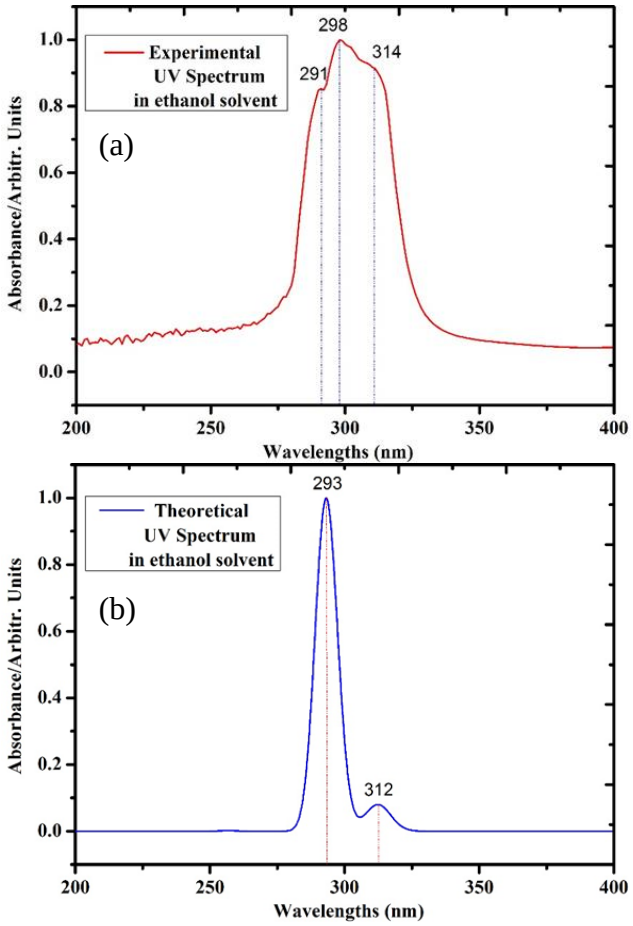

Figure 5 (a) The experimental and (b) the theoretical UV-Vis spectra of 1HBCM

4.4. Frontier Molecular Orbitals and Total, Partial and Population Density of States (DOS, PDOS and OPDOS)

The energy band gap in semiconductor materials is of great importance for electrical and optical studies [26]. The theoretical band gaps of 1HBCM are obtained by using the HOMO and LUMO energies. For electronic properties, the energy band was calculated using the TD-DFT method and determined which atoms are concentrated on it. The valence band (HOMO) was localized throughout the molecule except for the carboxylic acid and the monohydrate group, while the conductance band (LUMO) was localized throughout the molecule except for the monohydrate group.

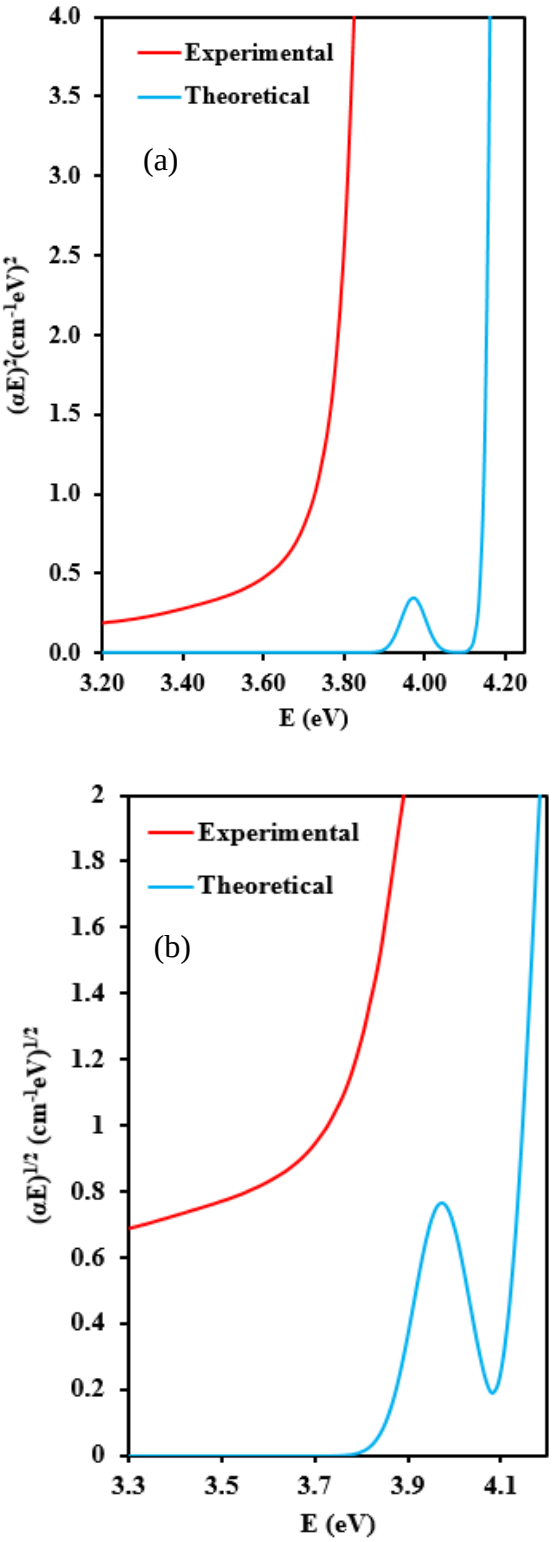

Figure 6 (a) Direct $((\alpha E)^2(cm^{-1}eV)^2$ vs photon energy) and (b) indirect $((\alpha E)^{1/2}(cm^{-1}eV)^{1/2}$ vs photon energy) band gap of 1HBCM

Table 3 Electronic values of the 1HBCM molecule.

DMSO			Theoretical Gas			Ethanol			Experimental (Ethanol)	
λ(nm)	E(eV)	f	λ(nm)	E(eV)	f	λ(nm)	E(eV)	f	λ(nm)	E(eV)
312.44 (46→48) (47→48) $\pi \rightarrow \pi^*$	3.9683	0.0433	312.22 (46→48) (47→48) $\pi \rightarrow \pi^*$	3.9710	0.0305	312.22 (46→48) (47→48) $\pi \rightarrow \pi^*$	3.9697	0.0417	314	3.9566
293.77 (46→48) $\pi \rightarrow \pi^*$	4.2205	0.5324	288.09 (46→48) $\pi \rightarrow \pi^*$	4.3036	0.4298	293.13 (46→48) $\pi \rightarrow \pi^*$	4.2296	0.5209	298	4.1605
256.38 (45→48) $\pi \rightarrow \pi^*$	4.8360	0.0010	267.11 (45→48) $\pi \rightarrow \pi^*$	4.6418	0.0010	256.69 (44→48) (45→48) $\pi \rightarrow \pi^*$	4.8302	0.0010	291	4.2693

Table 4 The calculated energy values and the energy gaps of 1HBCM)

Parameters	Gas	Ethanol	DMSO
E_{total} (Hartree)	-645.08	-645.091	-645.09
E_{HOMO} (eV)	-6.64	-6.79	-6.77
E_{LUMO} (eV)	-2.16	-2.29	-2.25
E_{HOMO-1} (eV)	-6.76	-7.03	-6.89
E_{LUMO+1} (eV)	-0.56	-0.42	-0.42
$E_{HOMO-LUMO\ gap}$ (eV)	**4.48**	**4.50**	**4.52**
$E_{HOMO-1-LUMO+1\ gap}$ (eV)	**6.20**	**6.61**	**6.47**
Chemical hardness (h)	2.24	2.25	2.26
Electronegativity (χ)	4.40	4.54	4.51
Chemical potential (μ)	-4.40	-4.54	-4.51
Electrophilicity index (ω)	4.32	4.57	4.50

Figure 7 also shows this localization. Using this figure, the energy band interval is calculated to be 4.48 eV and the detailed values are given in Table 4. Also, the values of chemical hardness, chemical potential, electrophilicity index and electronegativity are given in the table.

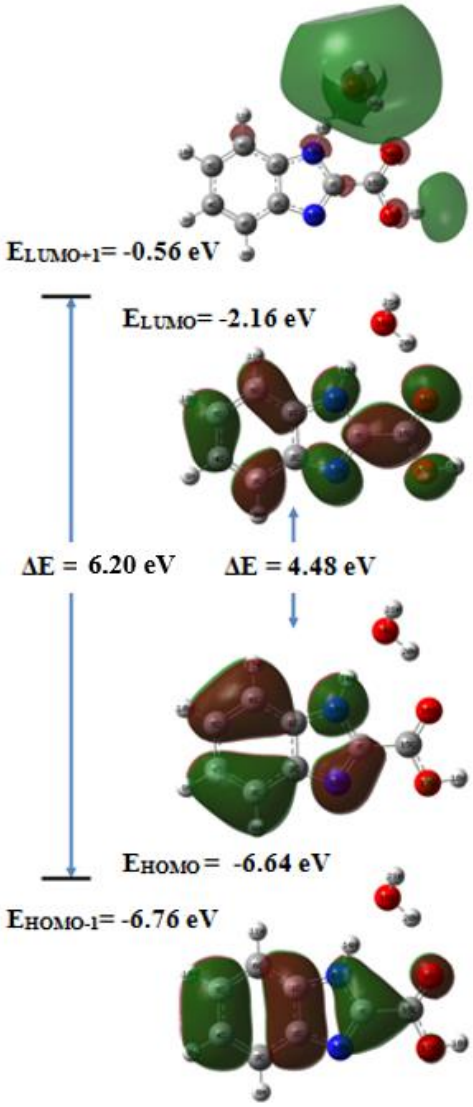

Figure 7 The frontier molecular orbitals of the 1HBCM for vacuum

The energy range of the molecule, i.e., the distance between the energy levels of the highest filled molecular orbital (HOMO) and the lowest empty molecular orbital (LUMO), and the total electronic density of states (TDOS or DOS) to show the interaction between the bonding, antibonding, and nonbonding orbitals, the density of states (PDOS), and the overlap population density of states (OPDOS or COOP) were calculated and generated using the GaussSum 2.2 program [27- 31].

The total electronic density of states (TDOS) displays the density spectrum of the molecule on the orbitals and is shown in Figure 8.

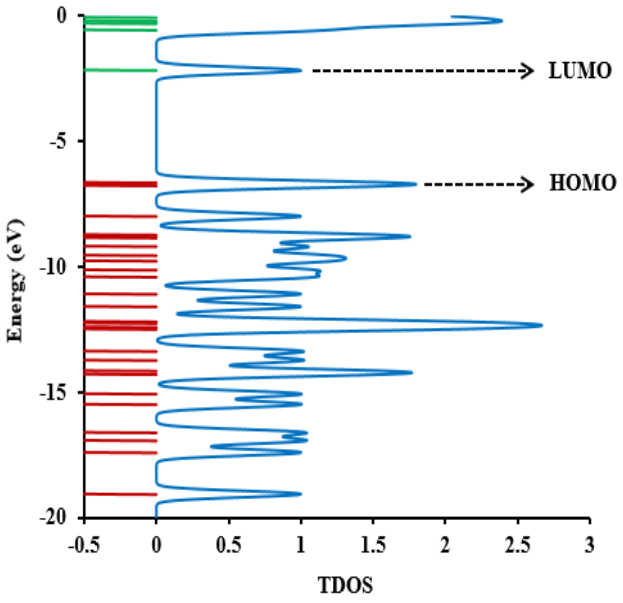

Figure 8 TDOS diagram of the 1HBCM in gas phase

In this spectrum, it can be seen which orbital has a higher electron density and HOMO-LUMO energy range can be calculated. For the molecule studied, the HOMO energy was calculated as -6.64 eV, the LUMO energy as -2.16 eV, and the energy range as 4.48 eV. In the TDOS spectrum, the red lines indicate the HOMO orbitals and the blue lines indicate the LUMO orbitals. The energy range chosen for these spectra is 0–20 eV.

The molecule studied was divided into 3 groups (benzimidazole, water, and carboxyl groups) and shown in Figure 9. The contribution of these groups to the HOMO-LUMO orbitals is shown in the figure.

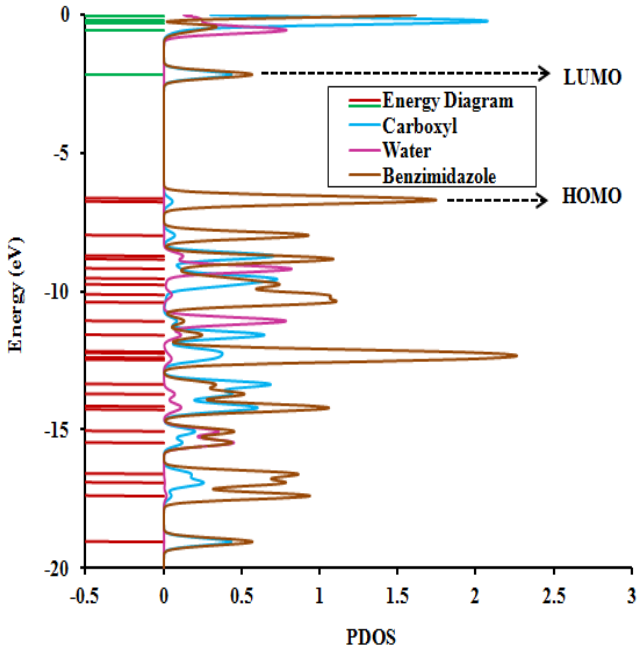

Figure 9 PDOS diagram of 1HBCM in gas phase

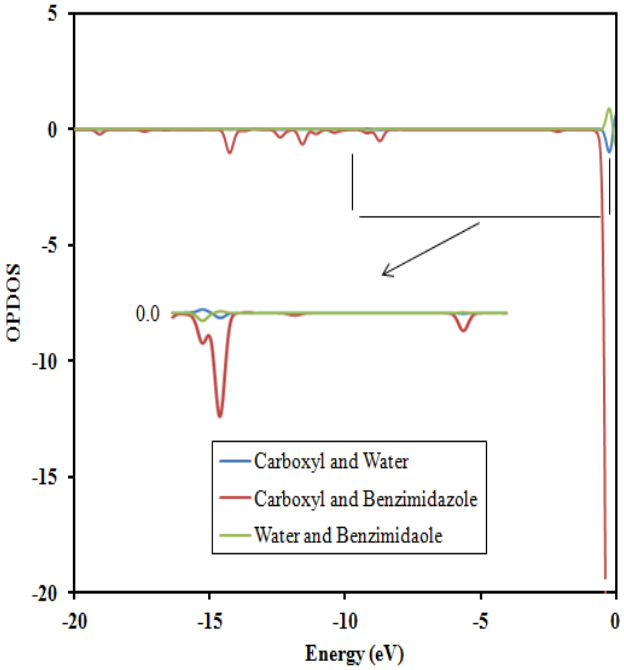

Figure 10 OPDOS diagram of 1HBCM in gas phase

The OPDOS spectrum shows the interaction of the bonding, anti-bonding, or non-bonding orbitals between two orbitals, atoms, or groups. Positive values in this spectrum indicate a bonding interaction (due to a positive overlap population), negative values indicate an anti-bonding interaction (due to a negative overlap population), and a value of zero indicates non-bonding interactions. [30]. The OPDOS diagram is shown in Figure 10 and can be easily identified

by the colors and values of the interactions between the selected groups. According to this diagram, the carboxyl-benzimidazole system (red) is negative, i.e., it has an anti-bonding character. However, the water-benzimidazole system (green) is positive, i.e. it shows a binding interaction.

4.5. Molecular electrostatic potential surface

The molecular electronic surface (MEP) shapes are a technique used to represent the electrophilic, nucleophilic, and neutral domains in the molecule [32-33]. These regions are represented as a function of the specific colors and the degrees of the colors. The color scale ranges from dark red to dark blue. The red areas represent the regions where the electrophilic reactions occur, that is, the electron-donating atoms, the blue areas represent the regions of the nucleophilic reactions, the electron-accepting atoms, the yellow colors and green, and the neutral areas.

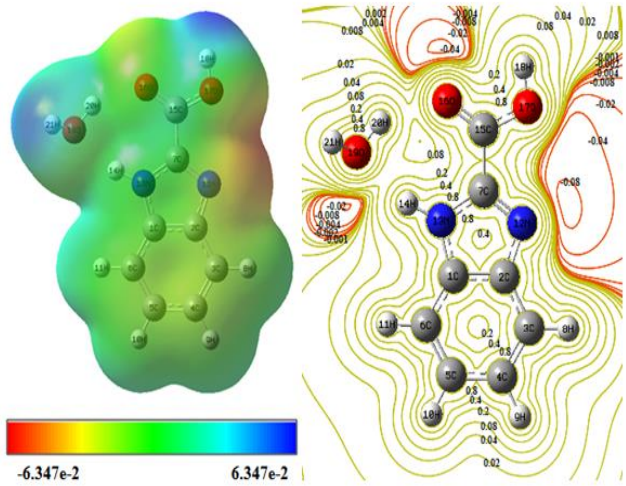

Figure 11 MEP map for 1HBCM molecules in gas phase

The electronic surface map for the 1HBCM molecule was found in the region of -6.347e2 and 6.347e2 (red to blue) and is shown in Figure 11. According to Figure 11, the nitrogen and oxygen atoms are the regions where the electrophilic reactions can occur in the molecule, and N11 is considered as the most electronegative atom in the molecule. The positive potential in the molecule was found at the hydrogen atoms in the monohydrate group. 2D peaks were drawn for the molecule and the red lines were concentrated around the electronegative atoms.

4.6. Mulliken atomic charges

Mulliken atomic charges are closely related to polarization, dipole moment, and acid-basic behavior of molecules. Since it plays an important role in quantum chemical calculations, it was calculated for this study as well, and the charge distribution was compared with the 1H-benzimidazole-2-carboxylic acid (1HBCA) molecule and given in Figure 12.

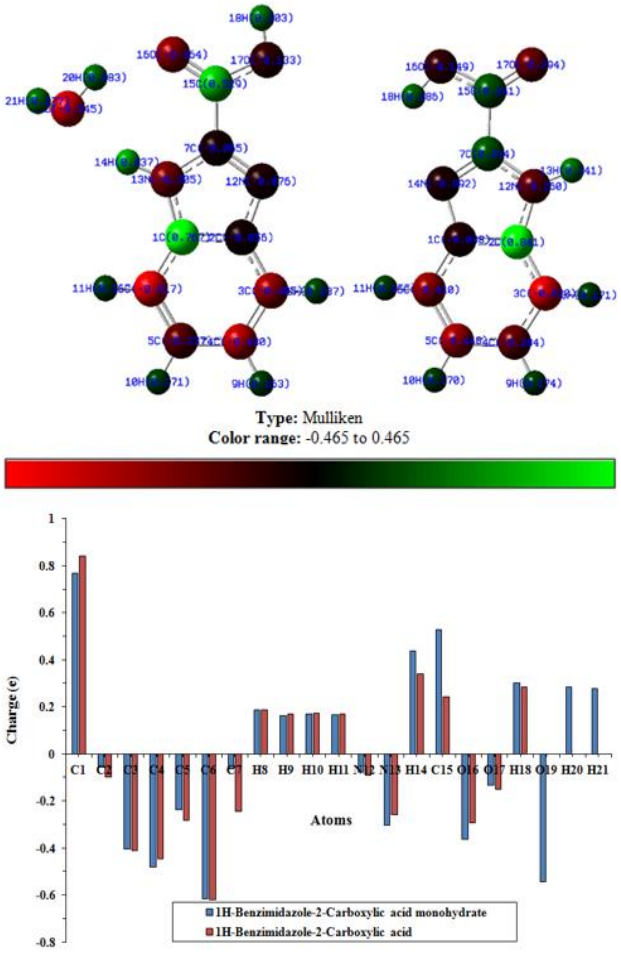

Figure 12 (a) In molecular form and (b) graphically the Mulliken charge distributions for 1HBCM and 1HBCA in gas phase

Looking at Figure 12, it is seen that the C1 atom has the highest positive value in both compounds (0.767 and 0.841 e). Although the C7 carbon atom is negative in both molecules, this value is smaller in the 1HBCM molecule. This difference

is thought to be due to the monohydrate group in the molecule.

4.7. Thermodynamic properties

Parameters such as entropy (S), enthalpy (H) and specific heat (C) can be used to predict new reactions of the molecule [34]. While investigating the minimum energy state of the 1HBCM molecule, the thermodynamic parameters of the molecule were also calculated. Since the vibrational properties of molecules increase with temperature [35- 36], these parameters were also investigated in 1HBCM molecule with temperature change. As shown in Figure 13, it is seen that the thermodynamic parameters increase with temperature and become stable at a certain temperature in accordance with the thermodynamic laws.

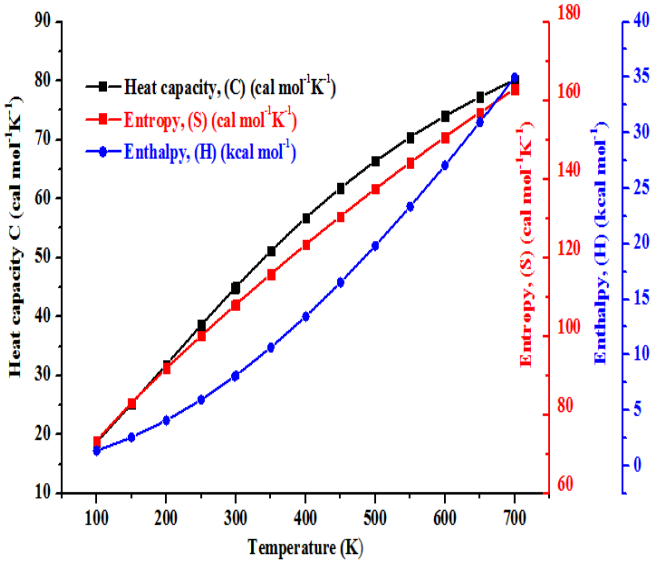

Figure 13 The correlation graphic of heat capacity, entropy, enthalpy and temperature for 1HBCM

5. CONCLUSION

As a result, the molecular structure, spectroscopic, optical and electronic properties of the 1HBCM molecule was investigated using experimental and quantum mechanical methods, and detailed information about these properties was given. The molecule was first optimized and the most suitable stable structure of the molecule was found. Geometric parameters and vibration spectra on the stable structure are given by comparing with similar molecules and experimental data. While the HOMO-LUMO band gap was calculated as 5.30 eV and 5.55 eV in similar molecules from the electronic properties of the molecule, this gap was calculated as 4.48 eV in 1HBCM molecule. When the Eg optical band gap values of the 1HBCM molecule were examined, it was observed experimentally as 3.68 eV (direct) and 3.57 eV (indirect). Considering the information presented, we hope that the usage areas of this structure will increase and that it will be used in health and semiconductor material applications.

Funding
This study is supported by Kırşehir Ahi Evran University Scientific Research Projects Coordination Unit. Project Number: TBY.A4.19.001.

Authors' Contribution
The authors contributed equally to the study.

The Declaration of Ethics Committee Approval
This study does not require ethics committee permission or any special permission.

The Declaration of Research and Publication Ethics
The authors of the paper declare that they comply with the scientific, ethical and quotation rules of SAUJS in all processes of the paper and that they do not make any falsification on the data collected. In addition, they declare that Sakarya University Journal of Science and its editorial board have no responsibility for any ethical violations that may be encountered, and that this study has not been evaluated in any academic publication environment other than Sakarya University Journal of Science.

REFERENCES

[1] W. Akhtar, M. F. Khan, G. Verma, M. Shaquiquzzaman, M. A. Rizvi, S. H. Mehdi, M. Akhter, M. M. Alam, "Therapeutic evolution of benzimidazole derivatives in the last quinquennial period" European Journal

of Medicinal Chemistry, vol. 126, no. 27, pp. 705-753, 2017.

[2] F. Fei, Z. Zhou, "New Substituted Benzimidazole Derivatives: a Patent Review (2010 - 2012)" Expert Opinion on Therapeutic Patents, vol. 23, pp. 1157–1179, 2013.

[3] M. Wang, X. Han, Z. Zhou, "New Substituted Benzimidazole Derivatives: A Patent Review (2013 - 2014)" Expert Opinion on Therapeutic, Patents no. 25, pp. 595–612, 2015.

[4] S. O. Podunavac-Kuzmonovic, L. M. Leovac, N. U. Perisicjanjic, J. Rogan, J. Balaz, "Complexes of cobalt(II), zinc(II) and copper(II) with some newly synthesized benzimidazole derivatives and their antibacterial activity" Journal of the Serbian Chemical Society, vol. 64, pp. 381-388, 1999.

[5] F. Vogetle, "Supramolecular Chemistry: An Introduction", Wiley, New York, 1991.

[6] K. Takahasi, K. Horino, T. Komura, K. Murata, "Photovoltaic Properties of Porphyrin Thin Films Mixed with *o*-Chloranil" Bulletin of the Chemical Society of Japan, vol. 66, no. 3, pp. 733–738, 1993.

[7] R. S. Mulliken, "Structures of Complexes Formed by Halogen Molecules with Aromatic and with Oxygenated Solvents" Journal of the American Chemical Society, vol. 72, pp. 600–608, 1950.

[8] A. M. Mansour, "Coordination behavior of sulfamethazine drug towards Ru(III) and Pt(II) ions: Synthesis, spectral, DFT, magnetic, electrochemical and biological activity studies", Inorganica Chimica Acta vol. 394, pp. 436–445, 2013.

[9] J. Tauc, A. Menth, "States in the gap" Journal of Non-Crystalline Solids, vol. 569, pp. 8–10, 1972.

[10] E. Babur Sas, M. Kurban, B. Gündüz, M.Kurt, "Photophysical, spectroscopic properties and electronic structure of BND: Experiment and theory", Synthetic Metals, vol. 246, pp. 39-44, 2018.

[11] S. Krawczyk, M. Gdaniec, F. Saczewski, "1H-Benzimidazole-2-carboxylic acid monohydrate" Acta Crystallographica Section E, vol. 61 pp. 4185-4187, 2005.

[12] E. B. Sas, M. Kurt, M. Karabacak, A. Poiyamozhi, N. Sundaraganesan, "FT-IR, FT-Raman, dispersive Raman, NMR spectroscopic studies and NBO analysis of 2-Bromo-1H-Benzimidazol by density functional method" Journal of Molecular Structure, vol. 1081, pp. 506–518, 2015.

[13] E. B. Sas, M. Kurt, "Ft-raman, ft-ir, nmr and dft calculations of 5-bromo-1h benzimidazole" Sakarya University Journal of Science, vol. 1, no. 3, pp. 430-441, 2017.

[14] M. Karabacak, E. Kose, A. Atac, E. B. Sas, A. M. Asiri, M. Kurt, "Experimental (FT-IR, FT-Raman, UV–Vis, 1H and 13C NMR) and computational (density functional theory) studies on 3-bromophenylboronic acid" Journal of Molecular Structure, vol. 1076, pp. 358–372, 2014.

[15] V. Krishnakumar, R. Ramasamy, "Density functional and experimental studies on the FT-IR and FT-Raman spectra and structure of 2,6-diamino purine and 6-methoxy purine" Spectrochim. Acta A, vol. 69, pp. 8-17, 2008.

[16] O. R. Shehab, A. M. Mansour, "Charge transfer complexes of 2-arylaminomethyl-1H-benzimidazole with 2,3-dichloro-5,6-dicyano-1,4-benzoquinone: Experimental and DFT studies", Journal of Molecular Structure, vol. 1047, pp. 121-135, 2013.

[17] N. T. A. Ghani, A. M. Mansour, "Molecular structure of 2-chloromethyl-1H-benzimidazole hydrochloride: Single crystal, spectral, biological studies, and DFT

calculations", Spectrochimica Acta Part A, vol. 86, pp. 605–613, 2012.

[18] T. S. Xavier, N. Rashid, I. H. Joe, "Vibrational spectra and DFT study of anticancer active molecule 2-(4-Bromophenyl)-1H-benzimidazole by normal coordinate analysis" Spectrochimica Acta Part A, vol. 78, pp. 319–326, 2011.

[19] V. Arjunan, A. Raj, C. V. Mythili, S. Mohan, "Structural, vibrational, electronic investigations and quantum chemical studies of 2-amino-4-methoxybenzothiazole" Journal of Molecular Structure, vol. 1036, pp. 327-340, 2013.

[20] G. Varsanyi, "Vibrational Spectra of Benzene Derivatives", Academic Press: New York, 1969.

[21] H. G. Silver, J. L. Wood, "Factors affecting torsional barriers in benzaldehyde derivatives", Transactions of the Faraday Society, vol. 60, pp. 5-11, 1964.

[22] R. Ramasamy, "Analysis of Vibrational Spectra of Pyridoxazinone Based on Density Functional Theory Calculations", Journal of Applied Spectroscopy, vol. 80, pp. 492–498, 2013.

[23] R. Ramasamy, "Vibrational spectroscopic studies of imidazole", Armenian Journal of Physics, vol. 8, pp. 51-55, 2015

[24] Y. Wang, R. A. Poirier, "Factors that influence the CN stretching frequency in imines", The Journal of Physical Chemistry A, vol. 101, no. 5, pp. 907–912, 1997.

[25] C. Y.Huang, T. Wang, F. Gai, "Temperature dependence of the CN stretching vibration of a nitrile-derivatized phenylalanine in water" Chemical Physics Letters, vol. 371, no. 5–6, pp. 731-738, 2003.

[26] I. Fleming, "Frontier Orbitals and Organic Chemical Reactions", Wiley, London, 1976.

[27] R. Hoffman, "Solids and Surfaces: A Chemist's View of Bonding in Extended Structures", Wiley- VCH Publisher, Newyork, 1988.

[28] W. Kohn, L. J. Sham, "Self-consistent equations including exchange and correlation effects" Physical Review, vol. 140, no. A, pp. 1133-1141, 1965.

[29] N. M. O'Boyle, A. L. Tenderholt, K. M. Langner "cclib: a library for package-independent computational chemistry algorithms" Journal of Computational Chemistry, vol. 29, pp. 839-845, 2008.

[30] S. Armaković, S. J. Armaković, J .P. Šetrajčić "Hydrogen storage properties of sumanene" International Journal of Hydrogen Energy, vol. 38, pp. 12190-12198, 2013.

[31] S. Armaković, S. J.Armaković, J. P. Setrajcic, S. K. Jacimovski, V. Holodkov, "Sumanene and its adsorption properties towards CO, CO_2 and NH_3 molecules" Journal of Molecular Modeling, vol. 20, pp. 2170-2177, 2014.

[32] N. Okulik, A. H. Jubert "Theoretical study on the structure and reactive sites of non-steroidal anti-inflammatory drugs" Journal of Molecular Structure: THEOCHEM, vol. 682, pp. 55-62, 2004.

[33] E. Scrocco, J. Tomasi, "Electronic molecular structure, reactivity and intermolecular forces: an euristic interpretation by means of electrostatic molecular potentials" Advances in Quantum Chemistry, vol. 11, pp. 115-193, 1978.

[34] H. P. Gümüş, Y. Atalay, "3-hidroksi-4-hidroksimiinometil-5-hidroksimetil-1,2-dimetilpiridinyum iyodid molekülünün geometrik yapısının incelenmesi" Sakarya University Journal of Science Institute, vol. 21, no. 3, pp. 564-571, 2017.

[35] J. B. Ott, J. Boerio-Goates, "Chemical Thermodynamics: Advanced Applications, Calculations from Statistical Thermodynamics", Academic Press, 2000.

[36] E. B. Sas, N. Cankaya, M. Kurt, "Synthesis of 2-(bis (cyanomethyl) amino)-2-oxoethyl methacrylate monomer molecule and its characterization by experimental and theoretical methods" Journal of Molecular Structure, vol. 1161, pp. 433-441, 2018.